Dehydroergosterol Structural Organization in Aqueous Medium and in a Model System of Membranes

Luís M. S. Loura and Manuel Prieto

Centro de Química-Física Molecular, Complexo I, Instituto Superior Técnico, 1096 Lisboa Codex, Portugal

ABSTRACT The aggregation of $\Delta^{5,7,9(11),22}$-ergostatetraen-3β-ol (dehydroergosterol or DHE), a fluorescent analog of cholesterol, was studied by photophysical techniques. It was concluded that the aqueous dispersions of DHE consist of strongly fluorescent microcrystals, and no evidence for self-quenching in micellar-type aggregates was found. The organization of DHE in model systems of membranes (phospholipid vesicles) is strongly dependent on the vesicle type. In small unilamellar vesicles, no evidence for aggregation is obtained, and the fluorescence anisotropy is rationalized on the basis of a random distribution of fluorophores. On the contrary, in large unilamellar vesicles (LUVs), a steeper concentration depolarization was observed. To explain this, a model that takes into account transbilayer dimer formation was derived. This was further confirmed from observation of excitonic absorption bands of 22-(N-7-nitrobenz-2-oxa-1,3-diazol-4-yl-amino)-23,24-bisnor-5-cholen-3β-ol (NBD-cholesterol) in LUV, which disappear upon sonication. It is concluded that, in agreement with recent works, sterol aggregation is a very efficient process in large vesicles (and probably in natural membranes), even at very low concentrations (~5 mol%).

INTRODUCTION

Cholesterol (structure depicted in Fig. 1) is a molecule of considerable biological importance and exists in large amounts in the membranes of animal cells. Its aggregation state is a relevant matter both in aqueous medium (regarding the study of cholesterol gallstones (Small, 1967; Chung et al., 1993) and atherosclerotic lesions (Small, 1970)) and in model systems of membranes (modulation of membrane properties; Rogers et al., 1979). Because cholesterol is nonfluorescent, informative techniques such as fluorescence and fluorescence anisotropy steady-state and time-resolved measurements, which could provide insight into this matter, are not applicable. Recently, with the increased availability of fluorescent analogs of cholesterol (Schroeder, 1984; Fischer et al., 1985), the use of these fluorescence techniques has become more common and useful in a variety of situations (Schroeder et al., 1991).

There are now several fluorescent molecules used as cholesterol analogs. Some of them do not occur naturally, and essentially consist of a cholesterol-like backbone labeled with a convenient fluorophore, e.g., the N-7-nitrobenz-2-oxa-1,3-diazol-4-yl-amino (NBD) -labeled derivatives, like the one depicted in Fig. 1, 22-NBD-23,24-bisnor-5-cholen-3β-ol (NBD-cholesterol), or the similar probe recently studied by Mukherjee and Chattopadhyay (1996). Although probes with good fluorescence properties can be synthesized, the extent to which they mimic cholesterol is not certain. In this respect, it is advantageous to use

intrinsically fluorescent sterols, which have structures almost identical to that of cholesterol. Examples of these are $\Delta^{5,7,9(11)}$-cholestatrien-3β-ol or cholestatrienol, and $\Delta^{5,7,9(11),22}$-ergostatetraen-3β-ol or dehydroergosterol (DHE). Their structures are depicted in Fig. 1.

Aqueous dispersions of cholesterol and fluorescent analog sterols have been little investigated, despite their above-mentioned relevance to common pathological situations. Renshaw et al. (1983) reported that cholesterol, when dispersed in an aqueous buffer, forms microcrystals of pure cholesterol and cholesterol monohydrate. Other structures have also been described, namely rodlike micelles (Castanho et al., 1992) and helical ribbonlike metastable intermediates (Chung et al., 1993) in different aqueous media. Rogers et al. (1979), who studied cholestatrienol aggregates in water, observed a strong fluorescence quenching, which was interpreted on the basis of nonfluorescent micelles. Hyslop et al. (1990) also reported a significant reduction in fluorescence intensity (<10% of that in ethanol solution) for the same molecule, apparently because of the formation of dark complexes, and ascribed the remaining emission to monomeric molecules (their emission spectrum being identical to that in ethanol). On the other hand, Schroeder et al. (1987) reported a large red shift (~50 nm) in the emission of DHE in water relative to that in 1-palmitoyl-2-oleoylphosphatidylcholine (POPC) vesicles (or organic solvents). This large difference could mean that, contrary to the cholestatrienol dispersions, the main fluorescent species in DHE is no longer the monomeric sterol; its nature remained unexplained.

Cholesterol analogs are, however, most frequently used in model membrane studies. Their association state can be suitably studied by monitoring the decrease in fluorescence anisotropy with increasing probe mole fraction. By using this technique and applying formalisms for depolarization by energy migration, one can readily determine whether
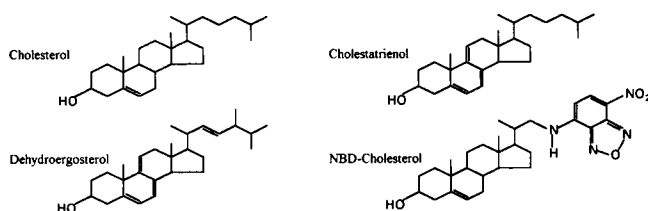
FIGURE 1 Structures of the cholesterol molecule and fluorescent cholesterol analogs.

molecules are randomly distributed in the membrane or, on the contrary, whether aggregation is taking place. Although a reasonable number of depolarization studies of these molecules incorporated in phospholipid vesicles have been performed (Schroeder et al., 1987; Hyslop et al., 1990; Smutzer, 1988; Butko et al., 1992), some controversy remains, both in the published data and in their interpretation. Schroeder et al. (1987) studied DHE in small unilamellar vesicles (SUVs) of POPC. Whereas the fluorescence lifetime was unaltered by increasing the DHE mole fraction (x_{DHE}), the steady-state anisotropy decreased sharply in the [x_{DHE} = 0.06, x_{DHE} = 0.08] range, being almost constant for x_{DHE} < 0.05 and x_{DHE} > 0.33. These results were interpreted on the basis of formation of sterol-rich domains in membranes (for a review, see Schroeder et al., 1991), but they were not ascribed to excitation energy homotransfer. On the other hand, Smutzer's results for DHE in dimyristoylphosphatidylcholine (DMPC) multilamellar vesicles (MLVs) at 20°C (Smutzer, 1988) show a sharp decrease for x_{DHE} < 0.05 (to ~70% the value at infinite dilution). Above this concentration, the anisotropy underwent only a slight decrease. These results were explained assuming interactions between DHE chromophores at low concentrations, whereas homotransfer was excluded as a possible cause for the concentration depolarization. The variance between Smutzer's results for MLVs and those of Schroeder et al. (1987) for SUVs could, according to the former author, be due to differences in surface curvature (much more pronounced in SUV) or formation (MLVs, unlike SUVs, would undergo osmotic compression because of solute exclusion upon formation) of these types of vesicles, which could induce differences in DHE packing. Butko et al. (1992) ascribe depolarization in POPC SUVs containing both DHE and cholesterol to homotransfer. However, these results were analyzed by using a hyperbolic equation derived for three-dimensional transfer geometry. Additionally, the fitting parameter is given only an empirical interpretation. For cholestatrienol and cholesterol/cholestatrienol mixtures in POPC liposomes, a quantitative study of concentration depolarization has been performed (Hyslop et al., 1990). No evidence for formation of sterol-rich domains was found for x(cholestatrienol) < 0.5.

In this work, after a preliminary report (Loura and Prieto, 1997), we address these two problems: 1) the true nature of DHE aggregates in aqueous medium (whether monomeric species, dark micelles, or microcrystals are formed) and 2)

a semiquantitative study of DHE concentration depolarization in two different model membrane systems, SUVs and large unilamellar vesicles (LUVs) of dipalmitoylphosphatidylcholine (DPPC), and at two different temperatures, 25°C (at which, for moderate DHE concentrations, the vesicles are in the $L_{\beta'}$ or gel phase) and 50°C (vesicles in the L_{α} or liquid crystalline phase). Regarding the unexpected anisotropy differences reported for the two types of vesicles, this study could provide insight into whether DHE aggregates are formed in either lipidic system, and in the former case, reveal the concentration at which aggregation becomes important.

MATERIALS AND METHODS

DHE was purchased from Sigma Chemical Co. (St. Louis, MO), and DPPC was obtained from Avanti Polar Lipids (Birmingham, AL). Both materials were used as received. Tris-HCl from BDH (London) was used to prepare the buffer (50 mM Tris-HCl, pH 7.4, 50 mM NaCl, 0.2 mM EDTA). NBD-cholesterol was purchased from Molecular Probes (Eugene, OR). NaCl (p.a.) and all organic solvents were from Merck (Darmstadt, Germany). Deionized water was used throughout.

The aqueous dispersions of DHE (final concentration ~6 × 10^{-5} M) were prepared either by the addition of small volumes of DHE solution in acetone to a given volume of buffer at 85°C (as described elsewhere; Castanho et al., 1992) or injection of small volumes (no more than 3% of total volume) of DHE solution in ethanol to buffer at room temperature. The two methods led to identical results.

DPPC MLV were prepared by mixing variable proportions of DHE and DPPC solutions in chloroform, followed by complete evaporation and hydration. SUVs were prepared by further sonication (carried out using a Branson Sonifier 250 fitted with a microprobe) and centrifugation as described elsewhere (Schroeder et al., 1987). For the preparation of LUVs, MLVs were extruded through two stacked polycarbonate filters (Nucleopore, 0.1-μm pore size) using an extruder (Lipex Biomembrane, Vancouver, Canada). The final DPPC concentration in both SUV and LUV samples was ~0.5 mM. The concentrations of the chloroform solutions of DPPC and DHE were determined by phosphorus analysis (McClare, 1971) and absorption ($\epsilon(\lambda_{max}$ = 327.8 nm) = 11200 M^{-1} · cm^{-1}; Smutzer et al., 1986), respectively.

All steady-state fluorescence measurements were carried out in a Spex F112 A Fluorolog spectrofluorimeter with a double emission monochromator. Excitation and emission spectra were made using 10 mm × 10 mm cuvettes in the aqueous medium studies and 5 mm × 5 mm cuvettes in the model membrane studies. To minimize photobleaching of DHE, narrow bandpasses in the excitation monochromator were used and, for the aqueous medium studies, gentle stirring was maintained inside the cuvette by a Hellma cuv-o-stir 333 magnetic stirrer. Under these conditions, fluorescence was largely independent of time, even when excitation was made at the absorption maximum. The bandwidths were 1.8 nm (excitation) and 2.25 nm (emission) for the spectra measurements, and 4.5 nm for both monochromators for the anisotropy measurements. All fluorescence measurements were carried out in a right-angle geometry. For the crystalline DHE spectra, polycrystalline powder was placed between two quartz plates, and a 30° geometry arrangement was used.

Fluorescence anisotropies were determined according to the equation (Lakowicz, 1983)

$$r = \frac{I_{VV} - G \cdot I_{VH}}{I_{VV} + 2 \cdot G \cdot I_{VH}}, \quad (1)$$

where I_{VV} and I_{VH} are fluorescence intensities, and the subscripts indicate the orientations of the excitation and emission Glan-Thompson polarizers, respectively. $G = I_{HV}/I_{HH}$ is the instrumental factor. Excitation and emission wavelengths were 324 and 376 nm, respectively. All intensities were

subtracted of the signal of an analogous vesicle preparation containing no fluorescent probe.

Fluorescence quantum yields were determined using anthracene in ethanol as the standard ($\Phi_F = 0.25$, determined from $\Phi_F = 0.27 \pm 0.03$ at 20°C for degassed solution; Eaton, 1988). Correction of excitation and emission spectra was performed using a rhodamine B quantum counter solution and a standard lamp, respectively (Eaton, 1988). The sample temperature was controlled to ±0.5°C.

Critical radii of energy homotransfer were calculated using a rewritten Förster's formula (Berberan-Santos and Prieto, 1987):

$$R_0 = 0.2108 \cdot \left[\kappa^2 \cdot \Phi_F \cdot n^{-4} \cdot \int_0^\infty I(\lambda) \cdot \epsilon(\lambda) \cdot \lambda^4 \cdot d\lambda \right]^{1/6},$$

(2)

where R_0 is expressed in Ångstroms, κ^2 is the orientational factor, Φ_F is the quantum yield of the probe, n is the refractive index of the medium, $I(\lambda)$ is the normalized emission spectrum, and $\epsilon(\lambda)$ is the molar absorption coefficient in $M^{-1} \cdot cm^{-1}$. Wavelength is expressed in nanometers. For the orientational factor, the value $\kappa^2 = 2/3$ (corresponding to a dynamic isotropic regime of transfer) was assumed, and $n = 1.4$ was considered.

Fluorescence decays were measured using the single photon timing technique (O'Connor and Phillips, 1984). The instrument was previously described (Farinha et al., 1994). Briefly, the excitation source was a nitrogen-filled lamp (Edinburgh Instruments 119F). Excitation ($\lambda = 337$ nm) and emission ($\lambda = 375$ nm) were selected with Jobin Yvon H20 monochromators. Decays were observed for three decades of intensity, with 0.122 ns/channel resolution, and 10,000 counts were accumulated in the peak channel. To avoid the color effect of the photomultiplier, data analysis was performed with the delta-function convolution method (Zuker et al., 1985), using p-bis(2-phenylozalyl)benzene in cyclohexane (degassed) as reference ($\tau = 1.1$ ns; Lampert et al., 1983). The quality of the fits was judged from the χ^2 parameter value and inspection of the weighed relative residuals and autocorrelation function plots.

Absorption spectra were recorded on a Jasco V-560 spectrophotometer. Circular dichroism (CD) measurements were carried out in a Jasco J-720 spectropolarimeter. Scanning electron microscopy (SEM) was carried out in a JEOL JSM-840 microscope using gold-coated samples, and for the optical observations a Zeiss Axioplan universal microscope was used.

RESULTS

Aqueous medium

In Fig. 2 the excitation and emission spectra of DHE in aqueous dispersions and in chloroform are shown. The determined quantum yield for DHE in this solvent ($\Phi_F = 0.002$) agrees with the published value of 0.003 (Smutzer et al., 1986). It is clear that although the spectra are similar in shape, there is a red shift in the aqueous dispersions' spectra. In the excitation spectrum, there are alterations in the vibronic profile, and the tail extending to the long wavelength region is more pronounced. The most remarkable changes are apparent in the emission spectrum. In addition to the monomeric fluorescence at 377 nm, a strong ($\Phi_F > 0.1$) and structured emission is observed at $\lambda_{max} = 427$ nm. This agrees with the results of Schroeder et al. (1987), confirming an interesting difference relative to the cholestatrienol dispersions, for which strong quenching is reported (Rogers et al., 1979; Hyslop et al., 1990). An identical spectrum is obtained from microcrystalline powder (see Fig. 2).
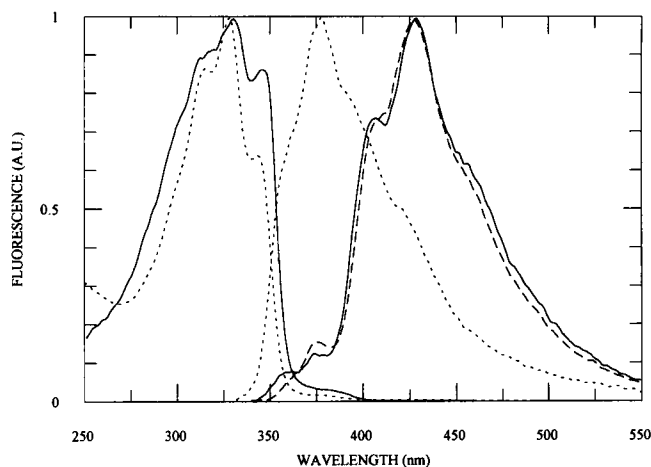
In Fig. 3 we compare the normalized spectra of DHE in

FIGURE 2 Corrected normalized fluorescence spectra of DHE. Shown are the emission spectrum of polycrystalline powder (- - -) and the excitation and emission spectra of buffer dispersion (———) and chloroform solution (· · · ·). For excitation spectra, the emission wavelength was fixed at 410 nm (CHCl$_3$ solution) and 475 nm (aqueous dispersion). For emission spectra, the excitation wavelength was fixed at 310 nm.

water before and after filtration through a 0.45-μm pore diameter filter. There are spectral changes in both excitation and emission, which indicate variation in the relative intensities of monomer and aggregate emission. Furthermore, a reduction in total fluorescence intensity upon filtration of ~50% was observed. However, no changes in the spectra were detected upon sonication.

Unlike DHE chloroform solutions (no CD detected; Yeagle et al., 1982b), aqueous dispersions exhibit strong CD, indicating a highly anisotropic environment. The CD spectrum (Fig. 4) is remarkably different from that of DHE
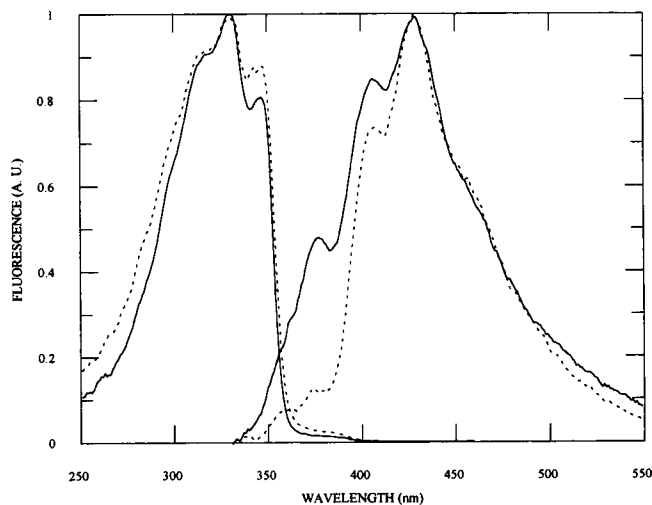

FIGURE 3 Corrected normalized fluorescence spectra of aqueous dispersion of DHE. Shown are the excitation and emission spectra before (· · · ·) and after (———) filtration through a 0.45-μm pore diameter filter. Conditions were the same as described in Fig. 2.
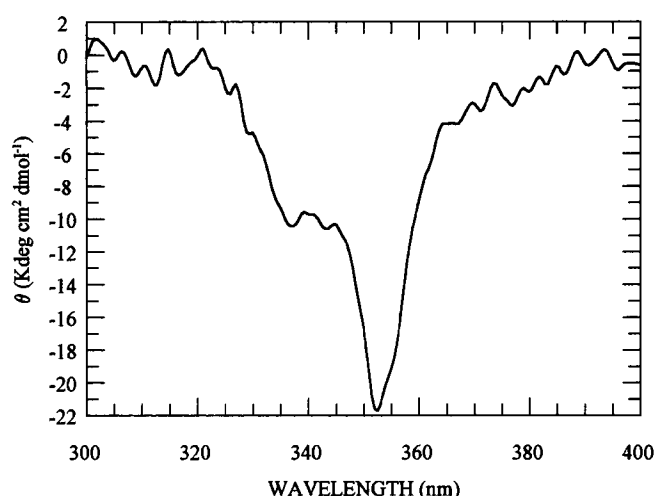
FIGURE 4   CD spectrum of DHE dispersion in buffer.

incorporated in membranes (Yeagle et al., 1982a), pointing to a different aggregation state.

Table 1 shows fluorescence decay data for DHE in chloroform, water, and crystalline state. The decays were complex, and acceptable values of the χ^2 parameter ($\chi^2 < 1.3$) required a biexponential fit. The average lifetime for the aqueous system is larger than that in chloroform by an order of magnitude, but is very similar to the value obtained for the crystals. Moreover, it is largely insensitive to temperature.

It has been reported (Castanho et al., 1992; Chung et al., 1993) that cholesterol molecules may aggregate into rodlike or ribbonlike structures in aqueous media, which could be large enough to allow observation by microscopic techniques. Fig. 5 shows SEM micrographs of a DHE/water sample. The white structures at the center of Fig. 5 A are probably DHE microcrystals. Although elongated shapes were occasionally observed (Fig. 5 B), the vast majority of the structures were relatively featureless.

Model systems of membranes (SUVs and LUVs)

The fluorescence excitation and emission spectra of DHE incorporated into DPPC vesicles (results not shown) are very similar to the ones depicted for chloroform (Fig. 2). There is a small but noticeable overlap of the spectra, which

TABLE 1   DHE fluorescence decay data*

	τ_1 (ns)	A_1[#]	τ_2 (ns)	$\langle\tau\rangle$ (ns)[§]
Chloroform solution	0.24	12.1	0.58	0.56
Polycrystalline powder	2.44	64.3	4.41	3.43
Aqueous dispersion				
(20°C)	3.05	72.9	5.09	3.83
(45°C)	2.66	66.5	4.67	3.60
(70°C)	2.21	62.4	4.16	3.25

*All decays were fit to a sum of two exponentials, $I(t) = A_1 \exp(-t/\tau_1) + A_2 \exp(-t/\tau_2)$.
[#]Normalized to 100%.
[§]Calculated as $(A_1\tau_1^2 + A_2\tau_2^2)/(A_1\tau_1 + A_2\tau_2)$.

yields Förster distances $R_0 = 13.3$ Å (25°C) and $R_0 = 11.5$ Å (50°C), in close agreement with the reported 13.2 Å for cholestatrienol in POPC (37°C, liquid crystal) (Hyslop et al., 1990). For these calculations (Eq. 2), we previously determined $\Phi_F = 0.13$ at 25°C and $\Phi_F = 0.05$ at 50°C and used Smutzer's value for the molar absorption coefficient in DMPC MLVs ($\epsilon = 3100$ M^{-1}·cm^{-1}, $\lambda = 326$ nm; Smutzer, 1988). The spectra and quantum yields were identical for both the SUV and LUV systems.

The variation in steady-state anisotropy r upon increasing DHE concentration is represented in Fig. 6. The anisotropies are normalized to the respective extrapolated values at infinite DHE dilution (0.28 for SUVs, 25°C; 0.24 for SUVs, 50°C; 0.30 for LUVs, 25°C; 0.28 for LUVs, 50°C). The theoretical homotransfer curves according to Snyder and Freire (1982) are also represented, for both 25°C and 50°C. These authors' Monte Carlo simulations assume depolarization by energy migration in a planar geometry (the curvature effect in the geometrical approximation from a spherical vesicle to a planar sheet is negligible when the sphere diameter D and the Förster radius R_0 obey the relationship $D/R_0 > 1.5$ (Eisinger et al., 1981), which is clearly the case), isotropic distribution of fluorophore absorption and emission dipoles, and a distance L of closest approach between molecules, which appears as a parameter in their model. We considered two different L values: 1) $L = 9.3$ Å, on the basis of atomic increments for the determination of the van der Waals radius (Edward, 1970) (L is taken as twice the van der Waals radius), and 2) $L = 7$ Å, after the value used by Hyslop et al. (1990) in their cholestatrienol study. At 25°C, the published model data (table 1 in Snyder and Freire, 1982) allow the calculation only for $L = 9.3$ Å. Average areas per phospholipid hydrophilic group (52.3 Å^2 at 25°C, 71.2 Å^2 at 50°C), which are necessary for computing the surface concentrations, were taken from Marsh (1990).

From Fig. 6 it is clear that the concentration depolarization curves of SUVs and LUVs are rather different. Whereas for SUVs a qualitative agreement is obtained (a better fit given by $L = 7$ Å), the anisotropy decrease in DHE in LUVs is steeper than expected. We questioned whether this was not due to light-scattering artifacts (Lentz et al., 1979). Because the LUV (or MLV) samples are more turbid than SUV samples for the same lipidic concentration, the measured anisotropy for the former systems could be artificially reduced. This decrease would be relatively more important for the concentrated samples, where anisotropy would already be small, even for SUV. The overall result for the curve of normalized anisotropy (r/r(infinite dilution)) of the turbid samples would be a shift to lower ordinates—hence the observed effect. To test this hypothesis, we measured the variation of anisotropy upon buffer dilution of both 10% DHE SUV and LUV lipidic systems. As can be seen in Fig. 7, the LUV anisotropy is always smaller than the SUV anisotropy, even for very small concentrations, so we believe that our concentration depolarization measurements are free from this artifact, and there seems to be a legitimate
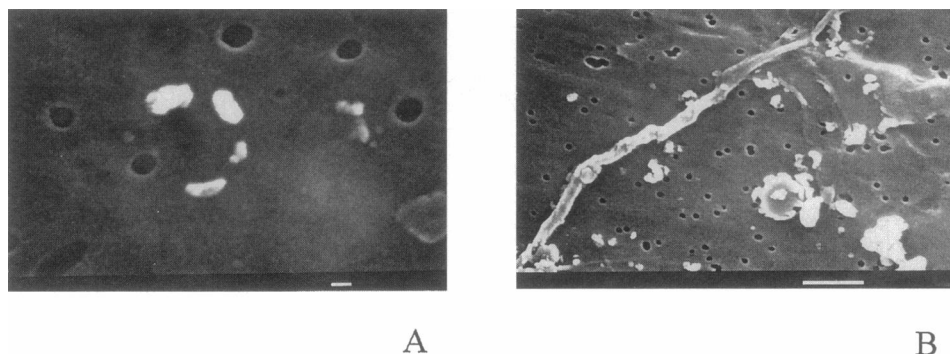
FIGURE 5 SEM micrographs of DHE dispersion in buffer. Small, irregularly shaped structures (microcrystals) were observed (*A*, scale bar = 100 nm), as well as rare ribbon-like structures (*B*, scale bar = 1 μm).

effect. Additionally, Fig. 7 shows that there is little advantage in diluting the samples below [DPPC] = 0.5 mM, because the anisotropy is almost invariant in the [0, 0.5 mM] DPPC concentration range. On the contrary, further dilution would lead to a low signal-to-noise ratio for the low DHE concentration samples, worsening the data quality.

DISCUSSION

Aqueous medium

The goal of the first part of this work was to understand the nature of DHE aggregates in water. Previous reports suggested either micelles with strong self-quenching (Rogers et al., 1979) or rodlike micelles (Castanho et al., 1992) for aqueous dispersions of cholestatrienol and cholesterol, respectively. From our experiments it is clear that DHE is highly fluorescent in water.

From the striking resemblance between the DHE/water and crystalline DHE emission spectra and lifetime data,

together with the microscopic studies, one can safely conclude that the DHE aggregates in water, which are the main fluorescent species, are microcrystals, and other possibilities (e.g., micellar aggregates) are excluded. The small emission at ~375 nm of the DHE emission spectra in water, characteristic of the emission in organic solvents, is due to "monomeric," solvated DHE. The differences in the fluorescence spectra obtained before and after filtration through 0.45-μm pore diameter filters are thus readily rationalized. Even though there are no visible alterations in the appearance of the sample, a considerable amount of DHE microcrystals is retained by the filter, and the filtrate is relatively enriched in monomeric DHE. The changes in the excitation spectrum are small, because the red shift in the excitation spectrum is small, ~5 nm. However, because the monomer and aggregate emission maxima are very far apart, this effect is clearly observed. The strong enhancement of the 375-nm (monomer) maximum relative to the absolute (aggregate) maximum reflects this increase in the ratio monomer/aggregate. The approximate twofold decrease in the total fluorescence maximum intensity shows that the aggregates are in fact large structures, their size being on the same
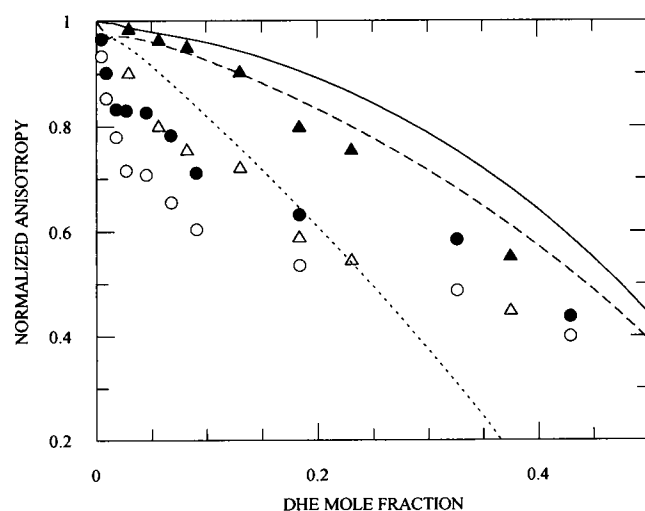

FIGURE 6 Normalized anisotropy (to infinite dilution) of DHE versus mole fraction in DPPC SUV at 25°C (●) and 50°C (▲), and DPPC LUV at 25°C (○) and 50°C (△). The lines are Monte Carlo simulations (Snyder and Freire, 1982) for L = 9.3 Å, 25°C (·····); L = 7 Å, 50°C (– – –) and L = 9.3 Å, 50°C (———) (see text). Average areas per phospholipid hydrophilic group (52.3 Å^2 at 25°C, 71.2 Å^2 at 50°C) were taken from Marsh (1990).
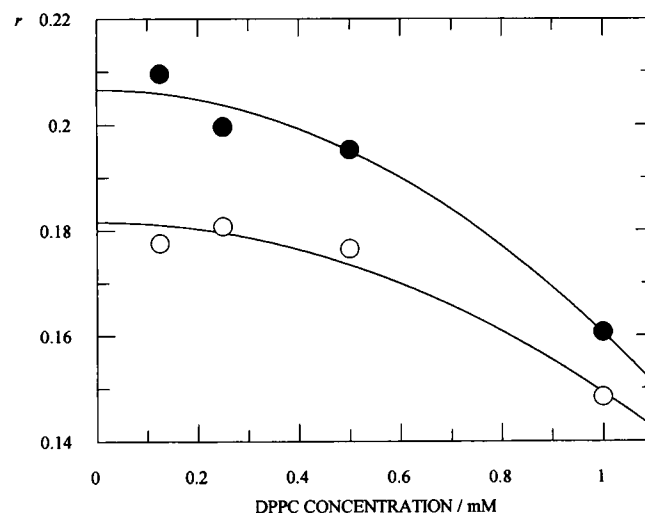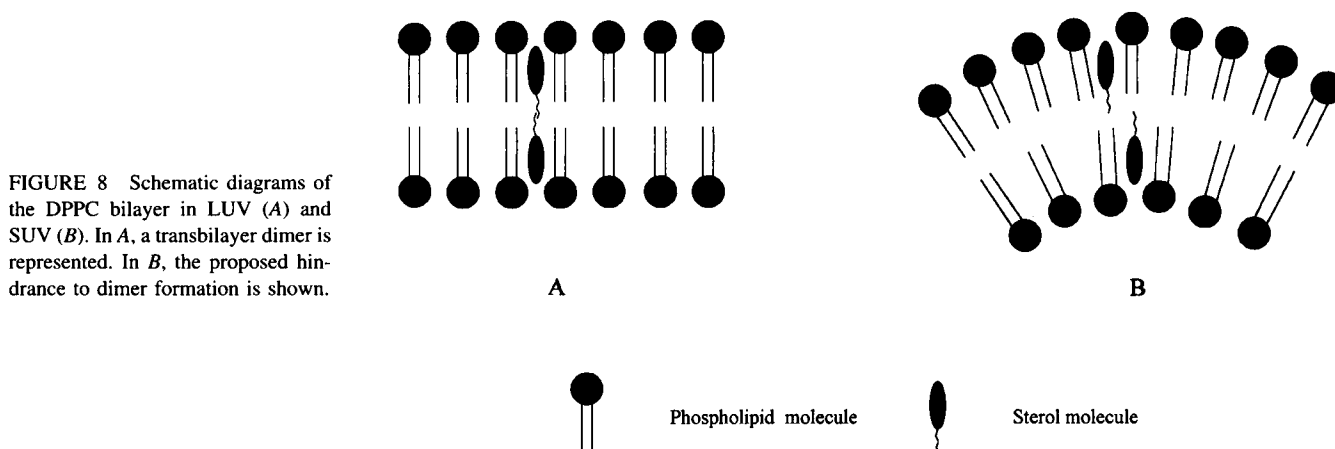

FIGURE 7 Variation of the anisotropy of DHE/DPPC vesicles (DHE 10 mol%) at 25°C as a function of lipid concentration for LUV (○) and SUV (●).

FIGURE 8 Schematic diagrams of the DPPC bilayer in LUV (A) and SUV (B). In A, a transbilayer dimer is represented. In B, the proposed hindrance to dimer formation is shown.

A   B

Phospholipid molecule   Sterol molecule

order of magnitude as that of the filter pores, which is confirmed by the SEM study (see Fig. 5). The observed microcrystals of DHE probably result from a series of transformations similar to those reported for cholesterol crystallization from bile, in which the system evolves from filamentous to helical and tubular microstructures in a time range of ~6 days (Chung et al., 1993). For DHE in buffer, thermodynamic equilibrium is probably attained much more rapidly.

Model systems of membranes (SUVs and LUVs)

The study of the anisotropy decrease upon increasing the DHE concentration in membranes was carried out to understand whether the observed depolarization could be rationalized assuming a random DHE distribution, or if, on the contrary, one should invoke aggregation (which could be characterized to some extent) to account for the observed effect. We studied two different types of vesicles, and at two distinct temperatures (above and below the main transition temperature for DPPC, $T_m = 41.4 \pm 0.5°C$; Marsh, 1990), to find out whether the vesicle type or phase influenced the DHE organization in the bilayer.

From comparison of the experimental SUV data with the theoretical expectations, we conclude that homotransfer provides an adequate explanation for the observed depolarization in this system. The difference between the SUV gel and SUV liquid crystal curves is readily rationalized using the homotransfer formalism, being due only to the smaller Φ_F (and hence R_0) value. The worse fit in the gel phase results probably arises from the used L value. In fact, $L = 7$ Å, the value used by Hyslop et al. (1990) in their cholestatrienol study, is probably a better estimate of the exclusion distance than the van der Waals diameter. As can be seen in Fig. 1, the structures of cholestatrienol and DHE are almost identical. Moreover, both are flat molecules, thus allowing a closer molecular packing than a spherical one of identical size. The SUV liquid crystal results further indicate that $L = 7$ Å gives a better fit, with more depolarization than $L = 9.3$ Å. The use of the former value in the gel phase plot

(prevented, as referred to above, by the lack of adequate model data in the Snyder and Freire article (1982)) would also shift the theoretical curve to lower ordinates closer to the experimental points.

The lines defined by the SUV data are quite smooth, with a lack of pronounced singularities (such as unexpected kinks, sudden drops followed by ranges of invariance, or the other way around), and are, in fact, similar in shape to the theoretical curves. The deviation observed at high DHE mole fractions ($x_{DHE} > 0.3$) is probably due to restricted rotational motion of the fluorophore, which would cause an incomplete loss of polarization, even at high concentrations (Lakowicz, 1983), at variance with the hypothesis of isotropic dipoles. Such partial immobilization (for example, rotational wobble of the fluorophore, instead of unrestricted motion) would result in a residual component both in anisotropy decays of the samples and in the concentration depolarization curve (Prieto et al., 1994).

The LUV results, on the other hand, show more pronounced depolarization than expected solely on the basis of energy migration. The Snyder and Freire (1982) curves lie above the experimental points, and a good fit would require the introduction of an interaction parameter (P in these authors' work), reflecting a tendency for the molecules to undergo self-aggregation (results not shown). This surprising effect is similar to the one described by Smutzer (1988), who compared his data for DMPC MLV with those of Schroeder et al. (1987) for POPC SUV. The former results show pronounced depolarization for 0–5% DHE, whereas the latter show little anisotropy decrease in the same range. As shown in Fig. 7, this is not due to light-scattering artifacts.

Although the organization of cholesterol and cholesterol derivatives in membranes at low fractions (<5%) has not been investigated at length, it was traditionally assumed that these molecules were essentially dispersed randomly in this concentration range, even though the evidence for it is not very clear (e.g., Estep et al., 1978; Vist and Davis, 1990; McMullen et al., 1993). However, more recently, Harris et al. (1995) studied the cryoscopic depression of MLVs of

DPPC/cholesterol (0–6% cholesterol) and explained their results on the basis of dimer formation in the fluid phase (and assuming insolubility in the gel phase) at low fractions (50% of total cholesterol would be dimerized at ~4.4 mol%). Based on space-filling considerations and analogous experiments for sterols lacking the isoprenyl chain, these authors proposed a transbilayer dimer arrangement (see Fig. 8 A), consistent with the earlier proposed deep location of cholesterol molecules across the nonpolar core of the two leaflets of the bilayer (Sankaram and Thompson, 1990, 1991). These dimers would form by hydrophobic interaction of the cholesterol tails. Interestingly, in lipid monolayers, where no transbilayer dimers can be formed, no evidence for cholesterol dimerization is observed (Albrecht et al., 1981). Mukherjee and Chattopadhyay (1996) invoked the same dimerization model to explain the observed spectral changes (more significantly in the absorption spectrum, with the appearance of an exciton band) of the NBD-labeled sterol 25-[N-[(7-nitrobenz-2-oxa-1,3-diazol-4-yl)-methyl]amino]-27-norcholesterol incorporated into LUVs at low fractions in both phases (0.5 mol% in the gel phase, 3 mol% in the fluid phase). Together, these recent reports indicate that cholesterol and cholesterol analogs could form dimers at low concentrations in MLVs and LUVs.

This prompted us to compare the measured DHE anisotropy in LUVs with a theoretical model that accounted for dimer formation. For a reversible equilibrium, we have

$$2[M] \leftrightarrows [D], \tag{3}$$

where M and D represent the monomer and dimer, respectively. Their concentrations are related by the dissociation constant, K_d,
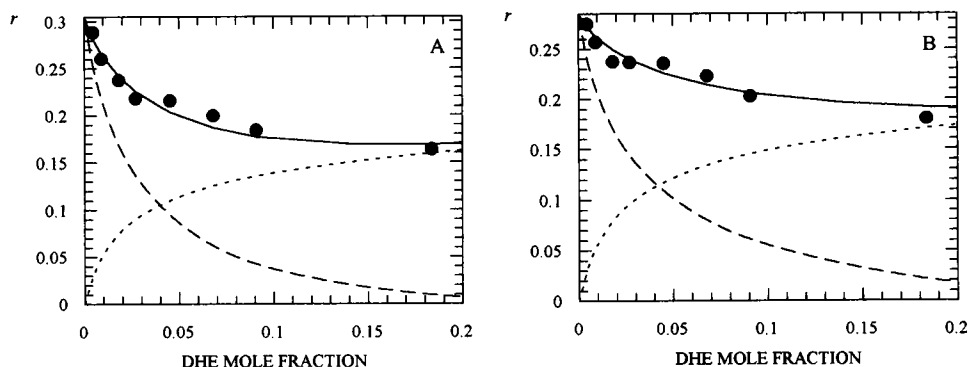
$$K_d = \frac{[M]^2}{[D]}. \tag{4}$$

In the Appendix we derive the approximate anisotropy curve for this system. The developed model considers energy migration among monomers, energy transfer between monomers and dimers (which act as traps for the excitation energy), and energy migration between the two sterol molecules of directly excited dimers. As shown in the Appendix, each curve has only three parameters, namely the

anisotropy value at infinite dilution (for which we used the same values as in the study assuming random distribution of molecules; Fig. 6), the dissociation constant (for which the recently reported value for cholesterol, obtained using a different method, $K_d = 0.044$ mol/mol DPPC (Harris et al., 1995) was used), and the distance R between the two individual fluorophores in the dimer. This was the only parameter optimized in our plots. Fig. 9 compares this model with the measured anisotropy in the 0–20 mol% range. The best fitting values were $R = 13.2$ Å for the gel phase and $R = 12.7$ Å for the liquid-crystalline phase data. A fair agreement (average deviation below 20 mol% DHE being <3%) is obtained in both phases, indicating that dimers are formed at low concentrations in DPPC/DHE LUVs, corroborating the results obtained for DPPC/cholesterol MLVs (Harris et al., 1995) and DPPC/25-[N-[(7-nitrobenz-2-oxa-1,3-diazol-4-yl)-methyl]amino]-27-norcholesterol LUVs (Mukherjee and Chattopadhyay, 1996). The R values indicate partial overlap of the aliphatic tail of the dimerized molecules, which also agrees with these authors' observations. The marginally smaller R value at 50°C may be related to the reduction in the bilayer width above the main transition temperature (e.g., Davenport et al., 1985, and references therein). This model, although not being accurate for the whole concentration range (see the Appendix), can adequately describe concentration depolarization when dimers are formed on a semiquantitative basis.

One could also try a two-parameter fit, to also recover the K_d constant. The best values in this case were $K_d = 0.031$ mol DHE/mol DPPC, $R_0 = 13.1$ Å, for the gel phase, and $K_d = 0.049$ mol DHE/mol DPPC, $R_0 = 12.7$ Å, for the liquid-crystalline phase. These K_d values for DHE are on the same order of magnitude as that reported for cholesterol (Harris et al., 1995), and used by us in the one-parameter fit. Moreover, the goodness of the fit does not improve considerably with this procedure. We therefore chose to optimize solely the interchromophoric distance R.

As further evidence for dimer formation in large vesicles, contrary to small vesicles, we prepared DPPC/NBD-cholesterol LUVs (2 mol% sterol) and compared the absorption spectrum at 25°C before and after sonication. In Fig. 10 we can see the excitonic band's splitting (at ~425 and ~513 nm, respectively) in the LUV spectrum (solid line), which

FIGURE 9 Variation of anisotropy of DHE in DPPC LUV at 25°C (A) and 50°C (B). The experimental data (●) are compared to the derived model curve (——). Also shown are the predicted monomer (– – –) and dimer (· · · ·) individual contributions to the global anisotropy. For the dimer, we considered $K_d = 0.044$ mol/mol DPPC (after the cholesterol value from Harris et al., 1995) and obtained $R = 13.2$ Å at 25°C and 12.7 Å at 50°C (see text).
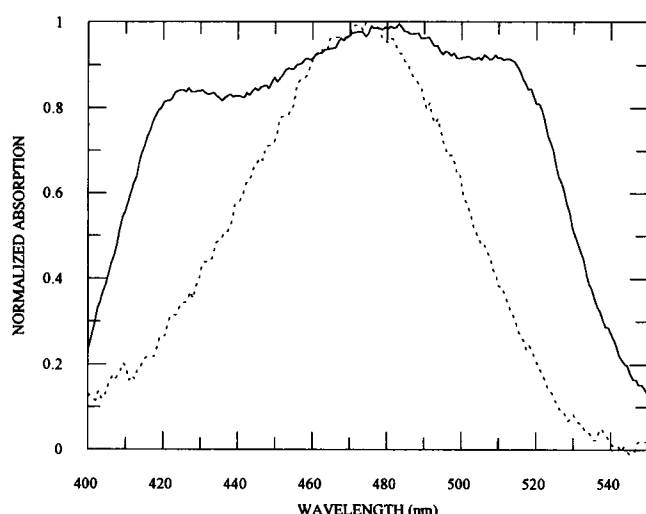
FIGURE 10 Normalized absorption spectra at 25°C obtained before (———) and after (· · · ·) sonication of NBD-cholesterol/DPPC (NBD-cholesterol 2 mol%) LUV.

maximum, only a slight inflection being noticeable. On the contrary, we observe a new band centered at about 513 nm, approximately as intense as the short wavelength peak. This indicates that the geometry of the exciton is different in the two cases. For 25-[N-[(7-nitrobenz-2-oxa-1, 3-diazol-4-yl)-methyl]amino]-27-norcholesterol, the longer aliphatic chain of the sterol probably constrains the two NBD chromophores to sit one above the other, in a stacked arrangement. In such a geometry, and provided the chromophores have approximate parallel or (as most probable in this case) antiparallel orientations, the longer wavelength excitonic transition is forbidden, in agreement with the reported spectrum. For NBD-cholesterol, we observed two intense bands, equidistant from the monomeric excitation maximum, the shift being ~ 2000 cm^{-1}. This probably means that the chromophores' dipoles are approximately coplanar and orthogonal, which could be due to the shorter aliphatic chain (there is no longer the stack constraint). Studies are currently under way to fully understand the geometry of this dimer.

CONCLUSIONS

This work addresses the problem of sterol aggregation, both in aqueous medium and when incorporated in phospholipid vesicles, as detected by fluorescence techniques. For this purpose the fluorescent DHE was used. It was concluded that the aqueous dispersions of DHE consist of strongly fluorescent microcrystals, ruling out the existence of dark micelles, as reported for another fluorescent sterol, cholestatrienol (Rogers et al., 1979). This was supported by the identity of fluorescence lifetime and emission spectra between the dispersions and the microcrystalline powder of the sterol. In addition, the relative intensities of monomer and aggregate change upon filtration of the suspension, and optical and electron microscopies revealed the appearence of the crystals.

The aggregation of DHE in membranes (DPPC LUVs and SUVs) was studied by measuring the variation in fluorescence anisotropy upon increasing the fluorophore concentration. This is due to an effective dipolar-type energy migration among the molecules. It was concluded that for SUVs, in both gel and liquid-crystalline phases, the results can be explained by assuming a random distribution of sterol. Surprisingly, for LUVs, the anisotropy decrease is much greater than expected on this basis. Following recent works that show evidence for effective sterol transbilayer dimerization, even at very low concentrations (Harris et al., 1995; Mukherjee and Chattopadhyay, 1996), a model was derived to predict depolarization in this aggregation regime and applied to the experimental data for LUVs.

In this way it was concluded that, for LUVs, dimer formation is an effective process at variance with SUVs. The prevention of transbilayer dimer formation in SUVs is assumed to be due to the strong bilayer curvature. Further support of this hypothesis was obtained from the observa-

disappears after sonication, leaving the known NBD monomer spectrum (dashed line). From exciton theory, the integrated absoption should remain the same upon excitonic interaction (e.g., see Cantor and Schimmel, 1980). We noticed a reduction of 25% in this absorption upon sonication, which could be due to some degradation of the molecule upon sonication or to incomplete separation of absorption from turbidity, but this is not critical to the discussion. SUVs are well known for their small size (25 nm for DPPC; New, 1990) and higher percentage of lipid in the outer monolayer (approximately 60–70%; Szoka and Papahadjopoulos, 1980). The fact that transbilayer dimers in LUVs are dissociated upon sonication is probably due to this monolayer asymmetry. The packing of solute molecules in the outer monolayer does not correspond directly to that of the inner monolayer, because the acyl tails of the outer monolayer lipid molecules do not match those of the inner molecules (see Fig. 8 B for a schematic representation). In this way, the tail-to-tail interactions between two solute molecules are hindered, and no exciton species is formed. The same probably holds for the DHE molecule. In this case, the tail-to-tail interaction is weaker, and no changes are verified in the spectra shapes. In any case, a dimerization process, similar to that reported by Harris et al. (1995) and Mukherjee and Chattopadhyay (1996), still occurs for large vesicles, but not for systems with lower curvature radius (SUVs)—hence the concentration depolarization differences.

Finally, we would like to briefly comment on the difference between the high-concentration absorption spectra obtained by us with NBD-cholesterol and those obtained by Mukherjee and Chattopadhyay (1996), using simple results from the exciton splitting quantum theory (e.g., see Cantor and Schimmel, 1980). These authors observed a new peak at about 430 nm, but in their reported spectra no major peak appears at longer wavelengths than the monomer absorption

tion of excitonic absorption (revealing dimer formation) of NBD-cholesterol in LUV. Upon sonication, the dimer is disrupted and a monomeric absortion, compatible with a random distribution, is observed. It can be concluded that in natural membranes, where no curvature effects are expected, dimer formation at very low concentrations (~5 mol%) is a very likely process.

APPENDIX

Anisotropy in a monomer/dimer system

Fluorescence anisotropy measurements reveal the angular displacement of the fluorophore that occurs between absorption and emission. In most situations, as rotational diffusion is important during the excited-state lifetime, there is a broadening of the angular distribution of emission dipoles due to rotation; hence the measured polarization is smaller than in a vitrified solution, in which rotation is negligible. If, furthermore, there is overlap between the absorption and emission spectra of the fluorophore(s), then Förster-type energy transfer can occur. As the donor and acceptor dipoles are generally not strictly parallel, each transfer process further contributes to broadening the angular distribution of emission dipoles, reducing the anisotropy. The greater the fluorophore concentration, the bigger the transfer probability and the anisotropy drop. Both transfer among identical fluorophores (homotransfer) and transfer to a different molecule (heterotransfer) may contribute to this depolarization, as long as there is spectral overlap and the acceptor fluorophores' concentration is high enough.

In a system where dimers (denoted by the subscript D) and monomers (denoted by the subscript M) coexist, the measured anisotropy has contributions from both entities. Considering that the anisotropy is additive (Lakowicz, 1983), we have

$$r = f_M r_M + f_D r_D, \qquad (A1)$$

with

$$f_i = \epsilon_i[i] \Phi_i g_i / \sum_j \epsilon_j[j] \Phi_j g_j, \qquad (A2)$$

where i, j = M or D; ϵ_i is the molar absorption coefficient; Φ_i is the fluorescence quantum yield; and g_i is the fluorescence intensity at the emission wavelength in a normalized spectrum. Because no spectral changes are observed for DHE, we considered $\epsilon_D = 2\epsilon_M$, $\Phi_D = \Phi_M$, and $g_D = g_M$. We have thus

$$f_M = [M]/([M] + 2[D]) \qquad (A3)$$

$$f_D = [D]/([M] + 2[D]). \qquad (A4)$$

Using the dissociation constant (Eq. 4) and introducing the mass balance equation,

$$T = [M] + 2[D], \qquad (A5)$$

where T is the total sterol concentration, we have

$$[M] = \frac{-0.5 + \sqrt{0.25 + 0.5 \, T/K_d}}{2/K_d} \qquad (A6)$$

and

$$[D] = (T - [M])/2, \qquad (A7)$$

so we can go back to Eqs. A3 and A4 and compute f_M and f_D.

Monomer anisotropy

The monomer anisotropy calculation must reflect the fact that there is depolarization due both to transfer to another monomer molecule and to a molecule that takes part in a dimer. Whereas in the former case there remains a significant probability of a further transfer step, either to the originally excited molecule or to a third one, in the latter case basically there is either decay to the ground state or transfer to the other molecule involved in the same dimer, transfer to other molecules having much smaller probability. In the following, these indirectly excited dimers are treated as energy traps (i.e., excitation transferred to them is lost). This assumption is discussed at the end of the Appendix.

The monomer anisotropy r_M can be calculated from the integrated emission components' decay functions,

$$r_M = \frac{\int_0^\infty I_{VV}(t)dt - \int_0^\infty I_{VH}(t)dt}{\int_0^\infty I_{VV}(t)dt + 2 \cdot \int_0^\infty I_{VH}(t)dt}, \qquad (A8)$$

where the different intensities are the time-resolved vertical and horizontal components of the fluorescence emission ($I_{VV}(t)$ and $I_{VH}(t)$, respectively) with excitation vertical to the emission axis.

Under simplifying assumptions (Sienicki et al., 1989, and references therein) the following set of equations applies:

$$I_{VV}(t) = \rho(t) \cdot [1 + 0.8 \cdot G^{s(t)}] \qquad (A9)$$

$$I_{VH}(t) = \rho(t) \cdot [1 - 0.4 \cdot G^s(t)]. \qquad (A10)$$

In these equations, $\rho(t)$ is the isotropic decay function, and $G^s(t)$ is the ensemble-averaged probability that an originally excited donor is still excited after time t (excluding the intrinsic decay). This function can be evaluated for integer dimensionality in a relatively simple manner, using the equation derived by Huber (1979) for two-component (donor and acceptor) systems:

$$G^s(t) = \exp[-\Gamma(1 - d/6)(2^{d/6-1}n_{dM}V_dR_{0MM}^d + n_{dD}V_dR_{0MD}^d) \cdot (t/\tau)^{d/6}], \qquad (A11)$$

where Γ is the complete gamma function, d is the Euclidean dimensionality of the system, n_{dM} is the number of donors (monomers in our case) per d-space volume unit, R_{0MM} is the donor-donor (monomer-monomer) Förster radius, n_{dD} is the number of acceptors (dimers) per d-space volume unit, R_{0MD} is the donor-acceptor (monomer-dimer) Förster radius, V_d is the d-dimensional unit sphere volume ($V_1 = 2$, $V_2 = \pi$, $V_3 = 4\pi/3$), and τ is the intrinsic donor fluorescence lifetime. In our system, we have $d = 2$ (two-dimensional system) and considered $R_{0MD} = 2^{1/6} \cdot R_{0MM}$ (from Eq. 2 and the assumed relationship $\epsilon_D = 2\epsilon_M$). We combined Eq. A11 with Eqs. A9 and A10, performed the integrations numerically, and r was calculated after substitution into Eq. A8. In this equation r(infinite dilution) = 0.4 is assumed. If this is not the case (as with our results), the calculated values should be multiplied by r(infinite dilution)/0.4.

Dimer anisotropy

Each directly excited dimer can be treated as an isolated pair of molecules (the distance between them being fixed), because the probability of transfer to a third molecule is much smaller than that of decay (either radiative or nonradiative) or transfer to the other molecule involved in the dimer. We used the following equation for a pair of molecules (Runnels and Scarlata, 1995):

$$r_D = r_1 \cdot \frac{1 + (R_{0MM}/R)^6}{1 + 2(R_{0MM}/R)^6} + r_2 \cdot \frac{(R_{0MM}/R)^6}{1 + 2(R_{0MM}/R)^6}, \qquad (A12)$$

where R is the distance between the two individual fluorophores within a dimer, r_1 is the anisotropy from the directly excited molecule, and r_2 is the anisotropy from the molecule that is excited by energy migration within the

dimer. If the absorption and emission dipoles in each molecule are parallel and the probes do not rotate, $r_1 = 0.4$ and r_2 (after a single energy transfer event) < 0.016 (Berberan-Santos and Valeur, 1991). If those conditions are not verified, the depolarization is even greater (Agranovich and Galanin, 1982). Here we take $r_1 = r$(infinite dilution) and $r_2 = 0.016 \cdot$ (r(infinite dilution)/0.4) (note that the second term always represents less than 4% of r_D, so that small inaccuracies in the r_2 value are not crucial).

Model assumptions

The main limitations to this model are the following:

1. It is assumed that dimers constitute traps to monomer excitation, and emission from indirectly excited dimers is neglected. Of course, these dimers should, in fact, emit, their anisotropy being very small (this should lead to less depolarization than measured).

2. Because Eq. A11 results from first-order truncation of the exact density expansion (Baumann and Fayer, 1986), no exclusion distance is considered in the calculation of r_M (this should lead to more depolarization than observed).

3. The calculation of r_M is based on the two-particle model proposed by Huber et al. (1977). This treatment considers the possibility of energy migration between the directly excited monomer to a second molecule (including backtransfer), but excludes all paths requiring more than two molecules (this should lead to less depolarization than observed).

4. Energy migration from one molecule involved in a dimer to another molecule, in monomeric form or involved in a second dimer, is neglected. (This should lead to less depolarization than measured at very high concentrations.)

The first point should be most important at moderate concentrations, where $r_M > r_D$, but dimer concentration is already high enough such that a photon-excited monomer has a significant probability of transferring its excitation energy directly to a dimer. The second and third effects should be most important in the same concentration range (where $r_M > r_D$, but T is already considerable). Note that, even though it is difficult to estimate errors, there is partial cancellation of deviations resulting from 1–3, and as these are only important in a narrow concentration range (~3–10 mol%), the recovery of a good fit in a broad concentration range is a criterion for the overall adequacy of the model. The last effect becomes significant only for very large concentrations (otherwise, transfer within the dimer or natural decay are much more probable than transfer to a third molecule). To avoid this effect, we restricted our analysis to less than 20 mol% DHE. In fact, using the above K_d value, we expect the average distance between two dimers in the gel phase for this concentration to be ~24 Å, so that transfer from a molecule in a dimer to a molecule in another dimer is about 18 times less probable than transfer within the dimer, whereas transfer to a monomeric molecule is even less probable.

REFERENCES

Agranovich, V. M., and M. D. Galanin. 1982. Electronic Excitation Energy Transfer in Condensed Matter. North-Holland Publishing, New York.

Albrecht, O., H. Gruler, and E. Sackmann. 1981. Pressure-composition phase diagrams of cholesterol/lecithin, cholesterol/phosphatidic acid, and lecithin/phosphatidic acid mixed monolayers: a Langmuir film balance study. J. Colloid Interface Sci. 79:319–338.

Baumann, J., and M. D. Fayer. 1986. Excitation energy in disordered two-dimensional and anisotropic three-dimensional systems: effects of spatial geometry on time-resolved observables. J. Chem. Phys. 85:4087–4107.

Berberan-Santos, M. N., and M. J. E. Prieto. 1987. Energy transfer in spherical geometry. Application to micelles. J. Chem. Soc. Faraday Trans. 2. 83:1391–1409.

Berberan-Santos, M. N., and B. Valeur. 1991. Fluorescence depolarization by electronic energy transfer in donor-acceptor pairs of like and unlike chromophores. J. Chem. Phys. 95:8048–8055.

Butko, P., I. Hapala, G. Nemecz, and F. Schroeder. 1992. Sterol domains in phospholipid membranes: dehydroergosterol polarization measures molecular sterol transfer. J. Biochem. Biophys. Methods. 24:15–37.

Cantor, C. R., and P. R. Schimmel. 1980. Biophysical Chemistry, Vol. 2. W. H. Freeman and Co., New York.

Castanho, M. A. R. B., W. Brown, and M. J. E. Prieto. 1992. Rod-like cholesterol micelles in aqueous solution studied using polarized and depolarized dynamic light scattering. Biophys. J. 63:1455–1461.

Chung, D. S., G. B. Benedek, F. M. Konikoff, and J. M. Donovan. 1993. Elastic free energy of anisotropic helical ribbons as metastable intermediates in the crystallization of cholesterol. Proc. Natl. Acad. Sci. USA. 90:11341–11345.

Davenport, L., R. E. Dale, R. H. Bisby, and R. B. Cundall. 1985. Transverse location of the fluorescent probe 1,6-diphenyl-1,3,5-hexatriene in model lipid bilayer membrane systems by resonance energy transfer. Biochemistry. 24:4097–4108.

Eaton, D. F. 1988. Reference materials for fluorescence measurement. J. Photochem. Photobiol. B Biol. 2:523–530.

Edward, J. T. 1970. Molecular volumes and the Stokes-Einstein equation. J. Chem. Educ. 47:261–269.

Eisinger, J., W. E. Blumberg, and R. E. Dale. 1981. Orientational effect in intra- and intermolecular long range excitation energy transfer. Ann. N.Y. Acad. Sci. 366:155–175.

Estep, T. N., D. B. Mountcastle, R. L. Biltonen, and T. E. Thompson. 1978. Studies on the anomalous thermotropic behavior of aqueous dispersions of dipalmitoylphosphatidylcholine-cholesterol mixtures. Biochemistry. 17:1984–1989.

Farinha, J. P. S., J. M. G. Martinho, H. Xu, M. A. Winnik, and R. P. Quirk. 1994. Influence of intrachain hydrogen bonding on the cyclization of a polystyrene chain. J. Polym. Sci. B Polym. Phys. 32:1635–1642.

Fischer, R. T., F. A. Stephenson, A. Shafiee, and F. Schroeder. 1985. Structure and dynamic properties of dehydroergosterol, $\Delta^{5,7,9(11),22}$-ergostatetraen-3β-ol. J. Biol. Phys. 13:13–24.

Harris, J. S., D. E. Epps, S. R. Davio, and F. J. Kézdy. 1995. Evidence for transbilayer, tail-to-tail cholesterol dimers in dipalmitoylglycerophosphocholine liposomes. Biochemistry. 34:3851–3857.

Huber, D. L. 1979. Donor fluorescence at high trap concentration. Phys. Rev. B. 20:5333–5338.

Huber, D. L., D. S. Hamilton, and B. Barnett. 1977. Time-dependent effects in fluorescent line narrowing. Phys. Rev. B. 16:4642–4650.

Hyslop, P. A., B. Morel, and R. D. Sauerheber. 1990. Oganization and interaction of cholesterol and phosphatidylcholine in model bilayer membranes. Biochemistry. 29:1025–1038.

Lakowicz, J. R. 1983. Principles of Fluorescence Spectroscopy. Plenum Press, New York.

Lampert, R. A., L. A. Chewter, D. Phillips, D. V. O'Connor, A. J. Roberts, and S. R. Meech. 1983. Standards for nanosecond fluorescence decay time measurements. Anal. Chem. 55:68–73.

Lentz, B. R., B. M. Moore, and D. A. Barrow. 1979. Light-scattering effects in the measurement of membrane microviscosity with diphenylhexatriene. Biophys. J. 25:489–494.

Loura, L. M. S., and M. Prieto. 1997. Aggregation state of dehydroergosterol in water and in a model system of membranes. J. Fluorescence. (in press).

Marsh, D. 1990. Handbook of Lipid Bilayers. CRC Press, Boca Raton, FL.

McClare, C. W. F. 1971. An accurate and convenient organic phosphorus assay. Anal. Biochem. 39:527–530.

McMullen, T. P. W., R. N. A. H. Lewis, and R. N. McElhaney. 1993. Differential scanning calorimetric study of the effect of cholesterol on the thermotropic phase behavior of a homologous series of linear saturated phosphatidylcholines. Biochemistry. 32:516–522.

Mukherjee, S., and A. Chattopadhyay. 1996. Membrane organization at low cholesterol concentrations: a study using 7-nitrobenz-2-oxa-1,3diazol-4-yl-labeled cholesterol. Biochemistry. 35:1311–1322.

New, R. R. C. 1990. Characterization of liposomes. *In* Liposomes: A Practical Approach. R. R. C. New, editor. Oxford University Press, Oxford. 105–162.

O'Connor, D. V., and D. Phillips. 1984. Time-Correlated Single Photon Counting. Academic Press, London.

Prieto, M. J. E., M. Castanho, A. Coutinho, A. Ortiz, F. J. Aranda, and J. C. Gómez-Fernandez. 1994. Fluorescence study of a derivatized diacylglycerol incorporated in model membranes. *Chem. Phys. Lipids.* 69: 75–85.

Renshaw, P. F., A. S. Janoff, and K. W. Miller. 1983. On the nature of dilute aqueous cholesterol suspensions. *J. Lipid Res.* 24:47–51.

Rogers, J., A. G. Lee, and D. Wilton. 1979. The organisation of cholesterol and ergosterol in lipid bilayers based on studies using non-perturbing fluorescent sterol probes. *Biochim. Biophys. Acta.* 552:23–37.

Runnels, L. W., and S. F. Scarlata. 1995. Theory and application of fluorescence homotransfer to melittin oligomerization. *Biophys. J.* 69: 1569–1583.

Sankaram, M. B., and T. E. Thompson. 1990. Modulation of phospholipid acyl chain order by cholesterol. A solid state deuterium nuclear magnetic resonance study. *Biochemistry.* 29:10676–10684.

Sankaram, M. B., and T. E. Thompson. 1991. Cholesterol-induced fluid-phase immiscibilty in membranes. *Proc. Natl. Acad. Sci. USA.* 88: 8686–8690.

Schroeder, F. 1984. Fluorescent sterols: probe molecules of membrane structure and function. *Prog. Lipid. Res.* 23:97–113.

Schroeder, F., Y. Barenholz, E. Gratton, and T. E. Thompson. 1987. A fluorescence study of dehydroergosterol in phosphatidylcholine bilayer vesicles. *Biochemistry.* 26:2441–2448.

Schroeder, F., J. R. Jefferson, A. B. Kier, J. Knittel, T. J. Scallen, W. G. Wood, and I. Hapala. 1991. Membrane cholesterol dynamics: cholesterol domains and kinetic pools. *Proc. Soc. Exp. Biol. Med.* 196: 235–252.

Sienicki, K., H. Itagaki, and W. L. Mattice. 1989. On the theory of concentration depolarization of fluorescence in one and two-component systems for multipole interactions in one, two and three dimensional medium. *J. Chem. Phys.* 91:4515–4521.

Small, D. M. 1967. Physicochemical studies of cholesterol gallstones formation. *Gastroenterology.* 52:607–610.

Small, D. M. 1970. Physical state of lipids of biological importance: cholesteryl esters, cholesterol, triglyceride. *Adv. Exp. Med. Biol.* 7:55–83.

Smutzer, G. 1988. A fluorescent sterol probe study of cholesterol/phospholipid membranes. *Biochim. Biophys. Acta.* 946:270–280.

Smutzer, G., B. F. Crawford, and P. L. Yeagle. 1986. Physical properties of the fluorescent sterol probe dehydroergosterol. *Biochim. Biophys. Acta.* 862:361–371.

Snyder, B., and E. Freire. 1982. Fluorescence energy transfer in two dimensions. A numeric solution for random and non-random distributions. *Biophys. J.* 40:137–148.

Szoka, F., and D. Papahadjopoulos. 1980. Comparative properties and methods of preparation of lipid vesicles (liposomes). *Annu. Rev. Biophys. Bioeng.* 9:467–508.

Vist, M. R., and J. H. Davis. 1990. Phase equilibria of cholesterol/dipalmitoylphosphatidyl choline mixtures: deuterium nuclear magnetic resonance and differential scanning calorimetry. *Biochemistry.* 29: 451–464.

Yeagle, P. L., J. Bensen, L. Boni, and S. W. Hui. 1982a. Molecular packing of cholesterol in phospholipid vesicles as probed by dehydroergosterol. *Biochim. Biophys. Acta.* 692:139–146.

Yeagle, P. L., J. Bensen, M. Greco, and C. Arena. 1982b. Cholesterol behavior in human serum lipoproteins. *Biochemistry.* 21:1249–1254.

Zuker, M., A. G. Szabo, L. Bramall, D. T. Krajkarski, and B. Selinger. 1985. Delta function convolution method (DFCM) for fluorescence decay experiments. *Rev. Sci. Instrum.* 56:14–22.